International Journal of Pattern Recognition
and Artificial Intelligence
Vol. 31, No. 3 (2017) 1750007 (13 pages)

DOI: 10.1142/S0218001417500070

Global and Local Oriented Edge Magnitude Patterns for Texture Classification

Jun Dong[*,†,‡,§,‖], Xue Yuan[¶,**] and Fanlun Xiong[*]

[*]*Institute of Intelligent Machines*
Hefei Institute of Physical Science Chinese Academy of Sciences
Hefei 230031, P. R. China

[†]*School of Information Science and Engineering*
Southeast University, Nanjing 210096, P. R. China

[‡]*Wuxi Zhongke Intelligent Agricultural Development Co., Ltd.*
Wuxi 21000, P. R. China

[§]*Jiangsu R&D Center for Internet of Things*
Wuxi 21000, P. R. China

[¶]*School of Electronic and Information Engineering*
Beijing Jiaotong University
No. 3 Shang Yuan Cun, Hai Dian District, Beijing, P. R. China
[‖]*djhf2003@hotmail.com*
[**]*xyuan@bjtu.edu.cn*

Received 18 May 2016
Accepted 11 July 2016
Published 21 September 2016

In this paper, we propose a gray-scale texture descriptor, name the global and local oriented edge magnitude patterns (GLOEMP), for texture classification. GLOEMP is a framework, which is able to effectively combine local texture, global structure information and contrast of texture images. In GLOEMP, the principal orientation is determined by Histogram of Gradient (HOG) feature, then each direction is respectively shown in detail by a local binary patterns (LBP) occurrence histogram. Due to the fact that GLOEMP characterizes image information across different directions, it contains very abundant information. The global-level rotation compensation method is proposed, which shifts the principal orientation of the HOG to the first position, thus allowing GLOEMP to be robust to rotations. In addition, gradient magnitudes are used as weights to add to the histogram, making GLOEMP robust to lighting variances as well, and it also possesses a strong ability to express edge information. The experimental results obtained from the representative databases demonstrate that the proposed GLOEMP framework is capable of achieving significant improvement, in some cases reaching classification accuracy of 10% higher than over the traditional rotation invariant LBP method.

Keywords: Texture classification; local binary pattern; histogram of gradient; rotation invariant.

1. Introduction

Texture analysis is currently an actively studied research topic in the fields of computer vision and pattern recognition. Generally, texture analysis involves four basic problematic issues: classifying images based on texture content; segmenting an image into regions of homogeneous texture; synthesizing textures for graphics applications; and establishing shape information from texture cues. Among these issues, texture classification has been the most widely studied, due to the fact that it has a wide range of applications, such as fabrics inspection, remote sensing, and medical image analysis, etc.

The local binary pattern (LBP) feature has emerged as a widely applied tool in the fields of texture classification and retrieval.[1,4–6,10,11,13,14,16] Ojala *et al.* first proposed the algorithm of LBPs.[14] Various extensions of the LBP has been proposed in the past decades, such as LBP variance with global matching (LBPVGM),[4] adaptive LBP (ALBP) algorithm,[6] LBP histogram Fourier features (LBP-HF),[1] Dominant LBP,[11] Completed LBP,[5] a pattern of oriented edge magnitudes (POEM),[16] local tetra patterns,[13] local quantization code (LQC),[22] completed robust local binary pattern (CRLBP),[23] and scale selective local binary patterns,[24] and so forth. LBPVGM is an alternative hybrid scheme, globally rotation invariant matching with locally variant LBP texture features. The scheme first estimate the principal orientations of the texture image, and then uses them to align LBP histograms. ALBP scheme uses the least square estimation to adaptively minimize the local difference for more stable directional statistical features. LBP-HF is a rotation-invariant image descriptor computed from discrete Fourier transforms of LBP histograms.

In addition, the current texture representations are combining or fusing different single features: LBP and Gabor features as in Refs. 20 and 21, LBP and SIFT (Scale-invariant Feature Transform) as in Refs. 3, 19 and 18, LBP and HOG as in Ref. 17. In Ref. 20, Zhang *et al.* introduced a combination approach extending LBP to local gabor binary pattern (LGBP) by applying multiorientation and multiscale Gabor filtering as a preprocessing step of LBP. They first calculate the 40 Gabor magnitude images, then apply the LBP method on these resulting images. This additional stage greatly improves performance when compared with the pure LBP algorithm. In a similar way, they proposed the histogram of Gabor phase pattern (HGPP)[21] combining the spatial histogram and the Gabor phase information encoding scheme. Unlike LGBP, HGPP encodes both real and imaginary images: it has to encode 90 images of the same size as the original one. These algorithms try to bring the advantages of different single features: the LBP method is a "micropattern" capturing image details at fine scales, whereas the Gabor filters are capable of characterizing image information over coarser scales and through different orientations. While the LBP method is good choice for describing texture information, the SIFT[12] and HOG approaches,[21,25,26] are widely accepted as the best feature to capture edge or local shape information. In Ref. 14, Ojala *et al.* indicated that it was possible to

regard image texture as a two-dimensional phenomenon characterized by two orthogonal properties, namely spatial structure (pattern) and contrast (the "amount" of local image texture). Spatial structure includes global structure information, local shape pattern, local texture pattern, etc. For instance, the HOG pattern detects global structure information, and the LBP detects micro-structures (e.g. edges, lines, spots and flat areas) the underlying distribution of which is estimated by means of a discrete occurrence histogram. Contrast is liable to be affected by illumination conditions, thus it is always represented by gradient magnitudes. Therefore, by combining the HOG, LBP and gradient magnitude features, it is possible to effectively represent a texture image. It is both a challenge and our motivation to determine a feature which satisfies both the criteria of distinctiveness and robustness. In this study, a novel texture descriptor is proposed, known as global and local oriented edge magnitudes patterns (GLOEMP), which is robust to both scale and rotation variations. In order to verify the effectiveness of proposed GLOEMP method, comparative experiments were performed. For this study, data from the public texture image database Outex, Contrib-TC and rotated texture images (RTIs) datasets are used. the experimental results show that the proposed GLOEMP feature is capable of yielding an excellent performance in terms of texture classification.

2. GLOEMP

In order to build rotation invariant features possessing distinctiveness, the authors propose applying the concept of calculating both the HOG-based structure, to describe the distribution of the holistic orientations and compensate the global-level rotation, and the LBP-based structure, to describe the distribution of local texture for each orientation. Then, the sequence of the holistic orientation is adjusted, and all histograms originate from its principal orientation. Based on the result of this step, all identical texture images may be considered to be on the same rotation. Finally, the LBP codes of each orientation are integrated based on the distribution of holistic edge information. The processing of building the GLOEMP is illustrated in Fig 1.

2.1. *Details of GLOEMP feature extraction*

The image gradient is computed, and the gradient orientation of each pixel is evenly discretized across $0^\circ - 360^\circ$. Then, a HOG is formed from the gradient orientations of the image, the HOG has K bins covering the 360° range of orientations. Each sample added to the histogram is weighted by its gradient magnitude. As shown in Fig. 2, exhaustive searching is used in the system to determine the rotation orientation with minimal distance between the template and test images, and this rotated orientation is assigned as the principal orientation θ_{main}. Then, all the bins of the histogram are shifted until the principal orientation shifts to the first position. It should be noted that the HOG is only used to determine the principal orientation and to adjust the distribution of the holistic orientations, and each orientation is respectively shown in detail by an LBP occurrence histogram.

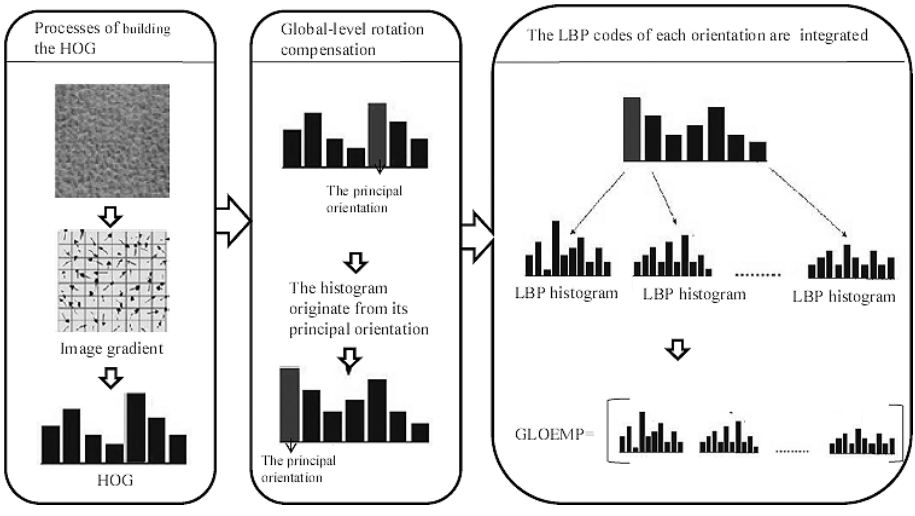

Fig. 1. Processes of building the GLOEMP.

Supposing the texture image is $M \times N$, after computing the image gradient and discretizing the orientation for each pixel, the entire image is represented by building a histogram, as follows:

$$H(\theta) = \sum_{x=1}^{M} \sum_{y=1}^{n} m(x, y) f(\theta_k, \theta_p), \quad k \in [1, k], \tag{1}$$

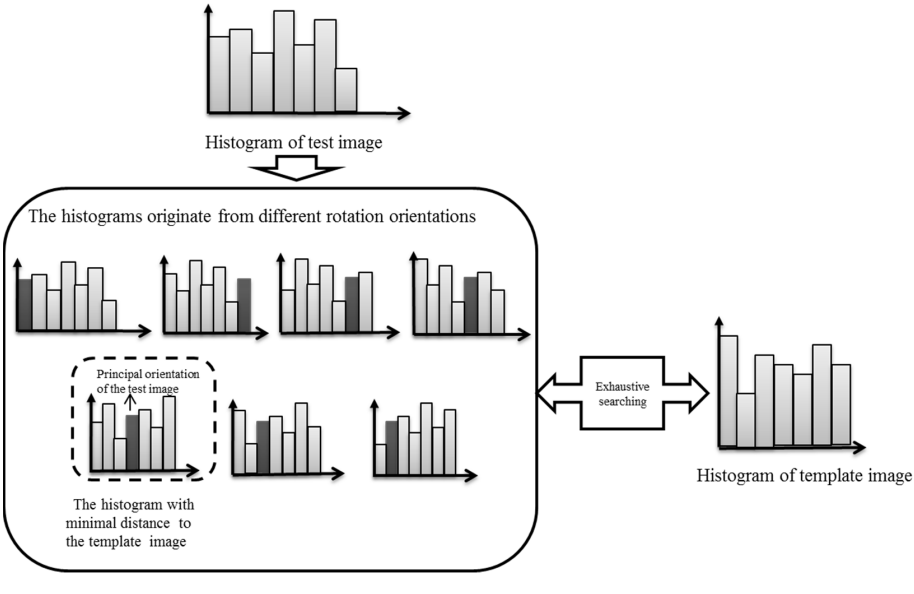

Fig. 2. Processes of determining the principal orientation θ_{main}.

where θ_P is quantified orientation of each pixel $P(x, y)$; K is the number of bins of the histogram; $m(x, y)$ is the gradient magnitude of pixel $P(x, y)$, and f is defined as follows:

$$f(a_1, a_2) = \begin{cases} 1 & \text{if } a_1 = a_2, \quad (2a) \\ 0 & \text{otherwise}, \quad (2b) \end{cases}$$

The second step is to compute LBP at each pixel. We use the notation to denote LBP feature, which is defined as:

$$\text{LBP}^{\text{riu2}}_{P,R} = \begin{cases} \sum_{P=0}^{P-1} s(g_p - g_c), & \text{if } U(\text{LBP}_{P,R}) \leq 2, \quad (3a) \\ P + 1 & \text{otherwise}, \quad (3b) \end{cases}$$

where

$$U(\text{LBP}_{P,R}) = |s(g_{p-1} - g_c) - s(g_0 - g_c)| + \sum_{P=0}^{P-1} |s(g_p - g_c) - s(g_{p-1} - g_c)|; \quad (4)$$

$$s(x) = \begin{cases} 1 & x \geq 0, \quad (5a) \\ 0 & x < 0, \quad (5b) \end{cases}$$

where g_c is the gray value of the central pixel; g_p is the value of its neighbors; P is the number of the neighbors; and R is radius of the neighborhood. Superscript riu2 reflects the use of rotation invariant uniform patterns which have U value of at most 2.

Finally, we build LBP histograms for each direction θ_k. This procedure is applied to the accumulated gradient magnitudes and across different directions to build the GLOEMP features. A GLOEMP feature is calculated for each discretized direction θ_k

$$\text{GLOEMP}^{\theta_k}_{P,R} = \sum_{x=1}^{M} \sum_{y=1}^{N} g(\theta_k, \theta) \text{LBP}^{\text{riu2}}_{P,\ R}, k \in [1, k], \quad (6)$$

where

$$g(a_1, a_2) = \begin{cases} m(x, y), & \text{if } a_1 = a_2, \quad (7a) \\ 0, & \text{otherwise}, \quad (7b) \end{cases}$$

where θ is the discretized direction of pixel (x, y) and $m(x, y)$ is the gradient magnitude of pixel (x, y).

The final feature is determined as follows:

$$\text{GLOEMP} = \{\text{GLOEMP}^{\theta_1}, \text{GLOEMP}^{\theta_2}, \ldots, \text{GLOEMP}^{\theta_k}\}. \quad (8)$$

2.2. *Properties of the GLOEMP feature*

For each pixel, GLOEMP characterizes not only local texture information, but also the relationships of the general distribution of the orientations. The feature possesses the following three properties:

(1) GLOEMP characterizes image information across different directions, thus it contains richer image information.
(2) GLOEMP uses gradient magnitudes as weight to add to the histogram, making it robust to lighting variance. In addition, GLOEMP has a strong ability to express edge information.
(3) The global-level rotation compensation method is proposed, which shifts the principal orientation of HOG to the first position, making GLOEMP robust to rotations. The former one property allow the features to convey rich image information, and the latter two properties allow the algorithm to be robust to exterior variations. There are various metrics to evaluate the goodness between two histograms, such as histogram intersection, loglikelihood radio, and chi-square statistic.[14] In this study, a test sample T is assigned to the class of model L that minimizes the chi-square distance:

$$D(T, L) = \sum_{X=1}^{X} (T_x - L_x)^2 / (T_x + L_x), \tag{9}$$

where X is the number of bins, and T_x and L_x are respectively the values of the sample and the model image at the xth bin.

3. Experiments

3.1. *Experiment setup*

In order to evaluate the effectiveness of the proposed method, a series of experiments were performed on three large and comprehensive public texture databases as shown in Fig. 3: the Outex database,[8] Contributed classification test suites (Contrib-TC) database and RTI dataset.[9,7] As a LBP based scheme, the proposed GLOEMP is compared with the representative LBP schemes in Ref. 14. Furthermore, we also compare GLOEMP with three state-of-the-art rotation invariant texture classification algorithms, the LBPVGM schemes in Ref. 4, the ALBP algorithm in Ref. 6 and the LBP-HF in Ref. 1. In the experiments, we also evaluate different combinations of two operators proposed, GLOBP and LOEMP. GLOBP has the same structure as GLOEMP, but it does not use gradient magnitudes as weight, thus Eqs. (7a) and (7b) were altered as follows:

$$g(a_1, a_2) = \begin{cases} 1, & \text{if } a_1 = a_2, \quad (10a) \\ 0, & \text{otherwise.} \quad (10b) \end{cases}$$

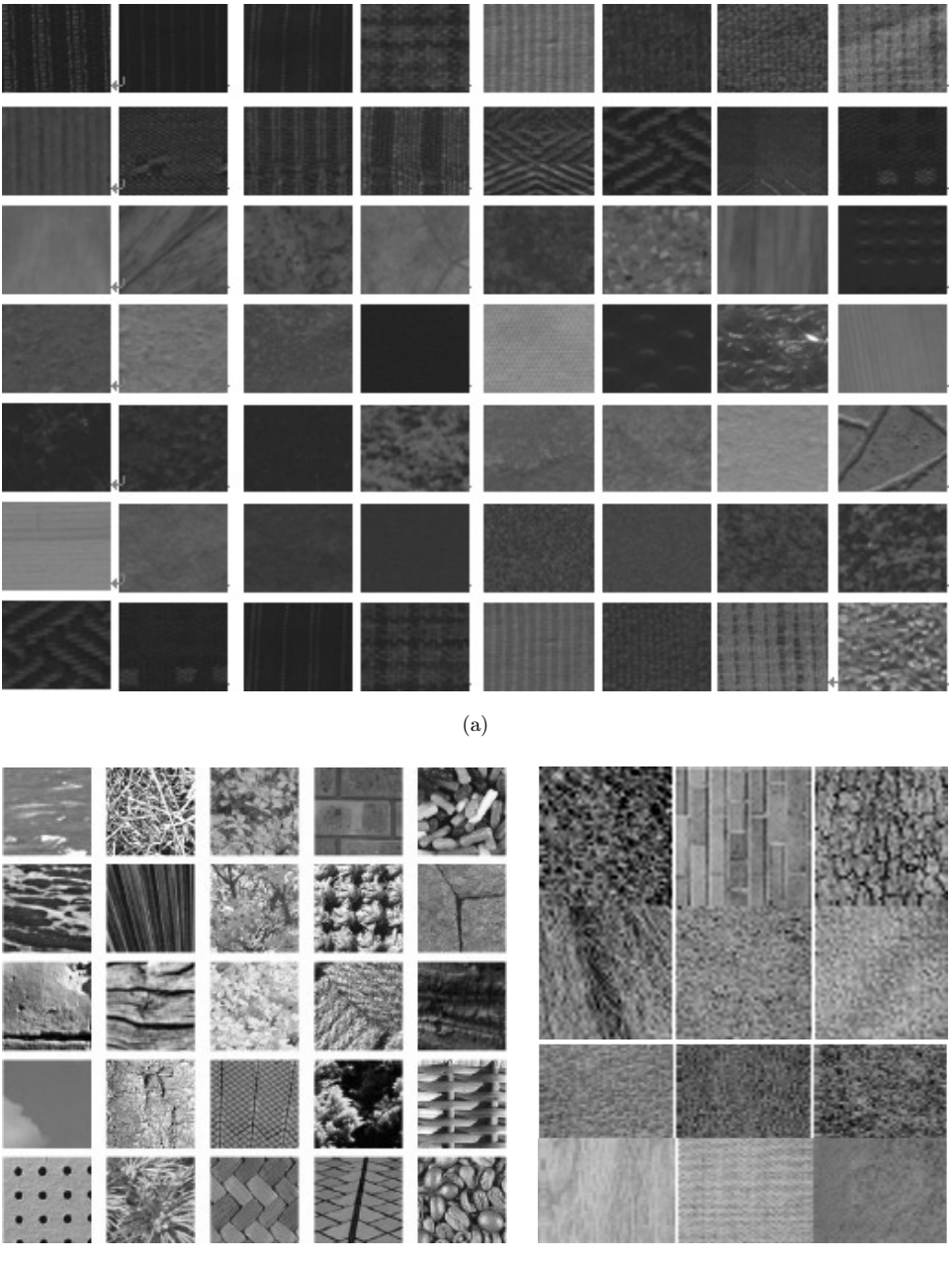

Fig. 3. Examples of texture samples for experiments: (a) examples from the Outex-TC-00014 dataset; (b) examples from the Contrib-TC-00006 dataset; (c) examples from RTI dataset.

3.2. *Experimental results*

3.2.1. *Experimental results on the Outex database*

The Outex-TC-00014 (TC14) dataset[8] is used in the experiments as shown in Fig. 3(a). The test suit contains 68 textures. In TC14, as test sample, two differently illuminated samples of the very same textures were utilized. The numbers of training and testing samples in this test were 680 and 1360, respectively.

For the number of bins of the HOG K, in this experiment K is set to 10 based on experience. The total $10 \times 28 = 280$ bins feature was used for GLOEMP8,1 and GLOEMP16,3. Recognition accuracies versus different K on the TC14 dataset are illustrated in Fig. 4(a), and the best recognition accuracy may be obtained when K is equal to 10 on the TC14 database. Table 1 lists the experimental results by different schemes. We could make the following findings:

- The GLOEMP achieves much better result than the GLOEP in most cases. It is in accordance with our analysis in Sec. 2.2 that the GLOEMP uses gradient magnitudes as weight to add to the histogram, making it robust to lighting variance. In addition, the GLOEMP has a strong ability to express edge information.
- The GLOEMP achieves better and more robust results than the state-of-the-art methods ALBP, LBP-HF and LBPVGM. It is due to the fact that GLOEMP combines both global structure information and local texture feature, and characterizes image information across different directions, it contains very abundant information, the GLOEMP feature is more distinctive than the other features.
- The GLOEMP is simple and fast to build the feature histogram, its feature size is smaller than that of the state-of-the-art methods: ALBP, LBP − HF and LBPVGM. For example, the dimension of the $\text{LBP}-\text{HF}_{8,1}^{\text{riu2}}$ is 326, and $\text{LBP}-\text{HF}_{16,3}^{\text{riu2}}$ is 73,766; the dimension of the $\text{LBPVGM}_{8,1}^{\text{riu2}}$ is 256 and the $\text{LBPVGM}_{16,3}^{\text{riu2}}$ is 65,536.

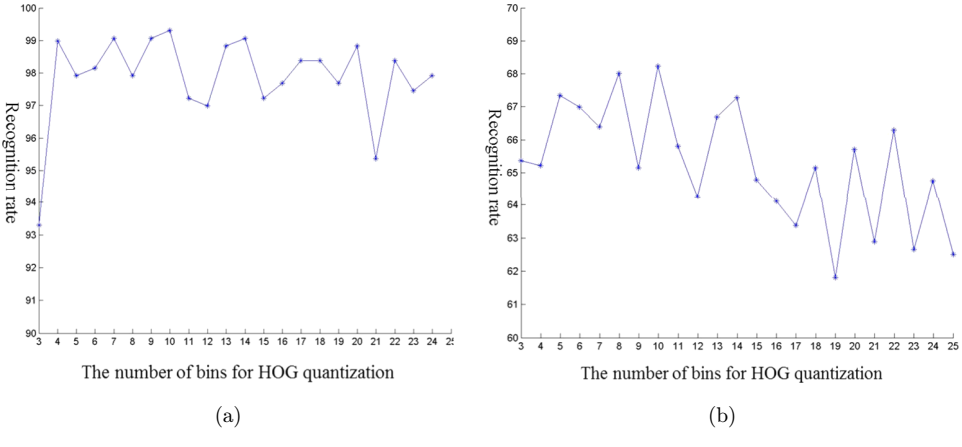

(a) (b)

Fig. 4. (a) Recognition rate versus different number of quantized orientation (k) on the TC14 dataset; (b) recognition rate versus different number of quantized orientation (k) on the TC6 dataset.

Table 1. Experimental results of comparative experiments on the Outex database.

P, R	(8,1)	(16,3)	(8,1)+(16,3)
$\mathrm{LBP}^{\mathrm{riu2}}_{P,R}$	43.38%	46.84%	57.94%
$\mathrm{GLOBP}^{\mathrm{riu2}}_{P,R}$	57.65%	58.75%	65.59%
$\mathrm{LBP-HF}^{\mathrm{riu2}}_{P,R}$	45.66%	39.34%	51.69%
$\mathrm{LBP-HF}^{U2}_{P,R}$	46.91%	53.82%	53.75%
$\mathrm{ALBP}^{\mathrm{riu2}}_{P,R}$	40.96%	46.99%	47.79%
$\mathrm{ALBP}^{U2}_{P,R}$	58.01%	58.46%	57.72%
$\mathrm{LBPVGM}^{\mathrm{riu2}}_{P,R}$	51.62%	8.09%	19.26%
$\mathrm{GLOEMP}^{\mathrm{riu2}}_{P,R}$	58.31%	59.26%	68.24%

- The GLOEMP is training free on feature extraction, and can still get good results when the training samples are limited.
- When multi-scale features ($\mathrm{GLOEMP}_{8,1}$ and $\mathrm{GLOEMP}_{16,3}$) are combined, the GLOEMP achieves more accurate results, and the improvement may be very significant.

3.2.2. *Experimental results on the Contrib-TC database*

In Contrib-TC-00006 (TC6),[8] the 54 VisTex textures were split into 128×128 sub-images as shown in Fig. 3(b). Since the size of the original images was 512×512, this makes up a total of 16 sub-images per texture. Half of the samples from each texture were used in training while the rest served as testing data. The number of training images from each class is 8, and the remaining eight images per class were used as the test set. The average accuracy over 20 randomly splits is listed in Table 2. The most ideal results are marked in bold font.

For the number of bins of the HOG K, in this experiment K is set to 10 based on experience; $\mathrm{LBP}^{\mathrm{riu2}}$ and $\mathrm{LBP}^{\mathrm{riu2}}$ used $10 + 18 = 28$ bins; and the total $10 \times 28 = 280$ bins feature was used for $\mathrm{GLOEMP}_{8,1}$ and $\mathrm{GLOEMP}_{16,3}$.

Table 2. Experimental results of comparative experiments on the Outex database.

P, R	(8,1)	(16,3)	(8,1)+(16,3)
$\mathrm{LBP}^{\mathrm{riu2}}_{P,R}$	84.03%	87.27%	87.27%
$\mathrm{GLOBP}^{\mathrm{riu2}}_{P,R}$	94.91%	96.76%	96.06%
$\mathrm{LBP-HF}^{\mathrm{riu2}}_{P,R}$	97.22%	88.19%	94.68%
$\mathrm{LBP-HF}^{U2}_{P,R}$	97.92%	92.82%	93.75%
$\mathrm{ALBP}^{\mathrm{riu2}}_{P,R}$	85.42%	86.81%	90.05%
$\mathrm{ALBP}^{U2}_{P,R}$	95.83%	93.98%	95.60%
$\mathrm{LBPVGM}^{\mathrm{riu2}}_{P,R}$	90.05%	29.17%	44.21%
$\mathrm{GLOEMP}^{\mathrm{riu2}}_{P,R}$	95.14%	96.76%	99.31%

Table 3. Experimental results of comparative experiments on the RTI dataset.

P, R	(8,1)	(16,3)
$\mathrm{LBP}^{\mathrm{riu2}}_{P,R}$	46.15%	52.75%
$\mathrm{GLOBP}^{\mathrm{riu2}}_{P,R}$	82.42%	100%
$\mathrm{LBP-HF}^{\mathrm{riu2}}_{P,R}$	79.12%	80.90%
$\mathrm{LBP-HF}^{U2}_{P,R}$	82.42%	98.90%
$\mathrm{ALBP}^{\mathrm{riu2}}_{P,R}$	89.01%	96.70%
$\mathrm{ALBP}^{U2}_{P,R}$	50.55%	56.04%
$\mathrm{LBPVGM}^{\mathrm{riu2}}_{P,R}$	38.46%	36.26%
$\mathrm{GLOBP}^{\mathrm{riu2}}_{P,R}$	94.51%	97.80%
$\mathrm{GLOEMP}^{\mathrm{riu2}}_{P,R}$	97.80%	100%

Recognition accuracies versus different K on TC6 dataset are illustrated in Fig. 4(b), and the best recognition accuracy may be obtained when K is equal to 10 on the Outex database.

Similar conclusions to those in Sec. 3.2.1 can be made from the experimental results on the TC6 dataset. The proposed GLOEMP gets better results than GLOEP for all cases.

3.2.3. *Experimental results on the RTI dataset*

The 13 texture images digitized from the Brodatz album and other sources (namely bark, brick, bubbles, grass, leather, pigskin, raffia, sand, straw, water, weave, wood and wool),[9,7] as shown in Fig. 3(b). The same set of seven different rotations was used: $0°, 30°, 60°, 90°, 120°, 150°$ and $200°$. Table 3 presents the results on RTI dataset using different methods. The most ideal results are marked in bold font.

Similar conclusions to those in Sec. 3.2.1 can be made from the experimental results on the TC6 dataset. The proposed GLOEMP gets better results than GLOEP for all cases. Furthermore, GLOEMP achieves better and more robust results than the state-of-the-art methods ALBP, LBP-HF and LBPVGM. It is due to the fact that the global-level rotation compensation method is proposed, which shifts the principal orientation of HOG to the first position, making GLOEMP robust to rotations.

4. Conclusions

In order to better represent the local texture, local shape and global structure information in texture images, this paper proposed a novel texture descriptor for texture classification, known as GLOEMP. Global structure was described by the HOG feature, and the distribution of the LBP pattern was used to describe the local texture pattern for each orientation. Based on the HOG feature, first the principal orientations of the texture image were estimated, then all the bins were shifted until the principal orientation shifted to the first position, in order to compensate for the

rotations of texture images. In addition, GLOEMP efficiently joined LBP and local gradient magnitudes, localedge magnitudes were computed and accumulated into the LBP bin. The experimental results on three large databases demonstrated that the proposed GLOEMP feature produces much higher classification accuracy than the traditional rotation invariant LBP and the other state-of-the-art methods. In future, more texture datasets such as UIUC, CUReT, KTH-TIP and real images will be used to verify the proposed algorithm.

Acknowledgment

This study was supported by the Natural Science Foundation of Jiangsu Province (No. BK20131090); the Six talent peaks project in Jiangsu Province (No. 2011-wlw-005); the National Natural Science Foundation of China No. 61301186.

References

1. T. Ahonen, J. Matas, C. He and M. Pietikäinen, Rotation invariant image description with local binary pattern histogram Fourier features, in *Proc. 16th Scandinavian Conf. Image Analysis (SCIA)* (2009), pp. 61–70.
2. N. Dalal and B. Triggs, Histograms of oriented gradients for human detection, in *Proc. CVPR* (2005), pp. 886–893.
3. M. Guillaumin, J. Verbeek and C. Schmid, Is that you? Metric learning approaches for face identification, in *Proc. ICCV* (2009), pp. 498–505.
4. Z. Guo, L. Zhang and D. Zhang, Rotation invariant texture classification using LBP variance with global matching, *Pattern Recogn.* **43**(3) (2010) 706–719.
5. Z. Guo, L. Zhang and D. Zhang, A completed modeling of local binary pattern operator for texture classification, *IEEE Trans. Image Process.* **19**(6) (2010) 1657–1663.
6. Z. Guo, D. Zhang, D. Zhang and S. Zhang, Rotation invariant texture classification using adaptive LBP with directional statistical features, in *17th IEEE Int. Conf. on Image Process. (ICIP)* (2010), pp. 285–288.
7. G. M. Haley and B. S. Manjunata, Rotation-invariant texture classification using a complate space-frequency model, *IEEE Trans. Image Process.* **8**(2) (1999) 255–269.
8. http://www.outex.oulu.fi/index.php?page=contributed.
9. http://www.ee.oulu.fi/research/img/texture/image-data/RotInv-13-6.html.
10. H. Lategahn, S. Gross, T. Stehle and T. Aach, Texture classification by modeling joint distributions of local patterns with Gaussian mixtures, *IEEE Trans. Image Process.* **19**(6) (2010) 1548–1557
11. S. Liao, M. W. K. Law and A. C. S. Chung, Dominant local binary patterns for texture classification, *IEEE Trans. Image Process.* **18**(5) (2009) 1107–1118.
12. D. G. Lowe, Object recognition from local scale-invariant features, *Proc. Int. Conf. Computer Vision.* pp. 1150–1157.
13. S. Murala, R. P. Maheshwari and R. Balasubramanian, Local Tetra Patterns: A new feature descriptor for content-based image retrieval, *IEEE Trans. Image Process.* **21**(5) (2012) 2874–2886.
14. T. Ojala, M. Pietikainen and T. Maenpaa, Multiresolution gray-scale and rotation invariant texture classification with local binary patterns, *IEEE Trans. Pattern Anal. Mach. Intel.* **24**(7) (2002) 971–987.

15. V. Perlibakas, Distance measures for PCA-based face recognition, *Pattern Recogn. Lett.* **25**(6) (2004) 711–724.
16. N. Vu and A. Caplier, Enhanced patterns of oriented edge magnitudes for face recognition and image matching, *IEEE Trans. Image Process.* **21**(3) (2012) 1352–1365.
17. X. Wang, Tony X. Han and S. Yan, An HOG-LBP human detector with partial occlusion handling, in *Proc. ICCV* (2009), pp. 32–39.
18. L. Wolf, T. Hassner and Y. Taigman, Similarity scores based on background samples, in *Proc. ACCV* (2009), pp. 88–97.
19. X. Yuan, J. Yu, Z. Qin and T. Wan, A SIFT-LBP image retrieval model based on bag-of-features, in *18th IEEE Int. Conf. on Image Process.* (2011).
20. B. Zhang, S. Shan, X. Chen and W. Gao, Histogram of Gabor Phase Patterns (HGPP): A novel object representation approach for face recognition, *IEEE Trans. Image Process.* **16**(1) (2007) 57–68.
21. J. Zou, Q. Ji and G. Nagy, A comparative study of local matching approach for face recognition, *Neurocomputing* **16**(10) (2007) 2617–2628.
22. Y. Zhao, R. Wang, W. Wang and W. Gao, Local quantization histogram for texture classification, *Neurocomputing* **207** (2016) 354–364.
23. Y. Zhao, W. Jia, R. Hu and H. Min, Completed robust local binary pattern for texture classification, *Neurocomputing* **106** (2013) 68–76.
24. Z. Guo, X. Wang, J. Zhou *et al.*, Robust texture image representation by scale selective local binary patterns, *IEEE Trans. Image Process.* **25**(2) (2016) 687–699.
25. Y.-T. Luo, L.-Y. Zhao, B. Zhang, W. Jia *et al.*, Local line directional pattern for palmprint recognition, *Pattern Recogn.* **50**(1) (2016) 26–44.
26. W. Jia, R.-X. Hu *et al.*, Histogram of oriented lines for palm print recognition, *IEEE Trans. on Systems Man and Cybernetics: Systems* **44**(3) (2014) 385–394.

Jun Dong received his Ph.D. from Nan Jing University of Posts & Telecommunations, Jiangsu, China. He is currently an Associate Researcher with the Institute of Intelligent Machines, Hefei Institute of Physical Science, Chinese Academy of Sciences, Hefei, China. His current research interests are in image processing, artificial intelligence and pattern recognition.

Xue Yuan received her M.S. degree and her Ph.D. from the Graduate School of Science and Technology of Chiba University, Chiba, Japan, in 2004 and 2007, respectively. In 2007, she joined SECOM Intelligent Systems Laboratory, Tokyo, Japan, as a researcher. In 2010, she joined the School of Electronics and Information Engineering, Beijing Jiaotong University, Beijing, China. Her current research interests are in image processing and pattern recognition.

Fanlun Xiong is currently a researcher at China University of Science and Technology of China. He was the International Federation of Automatic Control IFAC Fellow from 2006 to 2010, and member of China Automation Society. He has long been engaged in the research of intelligent technology and its application in machine vision, machine learning and data mining.